

Research report

Stable expression and characterization of the human brain potassium channel Kv2.1: blockade by antipsychotic agents

Barbara Wible^b, Michael K. Murawsky^a, William J. Crumb Jr.^c, David Rampe^{a,*}

^a Hoechst Marion Roussel, Inc., 2110 E. Galbraith Road, Cincinnati, OH 45215, USA

^b The Rammelkamp Center, Metro Health Campus and Department of Biochemistry, Case Western Reserve University, 2500 Metro Health Drive, Cleveland, OH 44109, USA

^c Department of Pediatrics, Tulane University School of Medicine, New Orleans, LA 70112, USA

Accepted 4 March 1997

Abstract

We have cloned the cDNA encoding the voltage-dependent K⁺ channel Kv2.1 from human brain (hKv2.1). RNase protection and RT-PCR (reverse transcriptase-PCR) experiments reveal abundant Kv2.1 transcripts in human brain with virtually no expression detectable in human heart. hKv2.1 has been stably transfected into a human glioblastoma cell line, and transformed cells display large, slowly activating outward currents. The kinetics, steady-state activation and inactivation parameters, and external tetraethylammonium sensitivity were all similar to those described previously for hKv2.1 channels transiently expressed in *Xenopus* oocytes or other mammalian cell lines. A number of dopamine receptor antagonist/antipsychotic agents were shown to block hKv2.1. Trifluoperazine, trifluoperidol and pimozide produced time-dependent blockade of hKv2.1 with IC₅₀ values of approx. 1–2 μM. The diphenylbutylpiperidine fluspirilene was shown to be 4–5-fold more potent than the other agents tested inhibiting hKv2.1 current with an IC₅₀ value of 297 nM. The block produced by fluspirilene was both time- and frequency-dependent. Furthermore, fluspirilene (1 μM) shifted the midpotential of the hKv2.1 steady-state inactivation curve by approx. 15 mV in the hyperpolarizing direction. These results demonstrate the usefulness of this transfection system for the pharmacological characterization of hKv2.1. Fluspirilene proved to be a relatively potent blocker of hKv2.1 and may provide a useful starting point for the development of more potent and selective agents active against this brain K⁺ channel.

Keywords: Potassium channel; Kv2.1; Antipsychotic agent; Fluspirilene; Human

1. Introduction

Voltage-dependent K⁺ channels play an important role in controlling electrical activity in excitable cells. As such, these channels play a dual pharmacological role as both important therapeutic targets on the one hand, and as sites for potentially lethal drug interactions on the other. Several distinct voltage-dependent K⁺ channels often co-exist in a particular cell. Furthermore, the biophysical and pharmacological properties of these channels can overlap making studies on a single channel subtype difficult. Fortunately, advances in molecular biology have led to the cloning of a wide number of K⁺ channel cDNAs [10,15]. For the most part, these clones have been transiently transfected into *Xenopus* oocytes or certain mammalian cell lines where

their functional properties can be elucidated. To date, far fewer of these cloned channels have been stably transfected into immortalized cell lines. Such stably transfected cells offer advantages over their transient counterparts, especially where large numbers of channels may be required on a continuous basis.

The voltage-gated K⁺ channel Kv2.1 is a member of the Shab subfamily [5,10]. The cDNA of Kv2.1 encodes a slowly activating, non-inactivating type of K⁺ channel current. In species such as rat, abundant transcripts for the Kv2.1 channel exist in both brain and heart [3]. This tissue distribution suggests that Kv2.1 may be an attractive target for the development of drugs for both neurological and cardiovascular disorders, respectively. In the present study, we describe the cloning and stable expression of human Kv2.1, compare its mRNA levels in human brain and heart and detail the effects of various antipsychotic agents on this channel.

* Corresponding author. Fax: +1 (513) 948-6439.

2. Materials and methods

2.1. Cloning and expression of hKv2.1

A partial cDNA clone of hKv2.1 was isolated from a human fetal brain cDNA library in λ gt10 (Clontech, HL1065a) by screening with 32 P-random prime-labeled rat Kv2.1 cDNA fragments. This clone encoded the carboxyl-terminal portion of hKv2.1 (amino acids 304–858) beginning at the *EcoRI* site in the middle of the putative S4 transmembrane segment through the stop codon following the terminal isoleucine residue. Sequencing of this cDNA fragment showed that it was identical to the hKv2.1 gene cloned from a human genomic cDNA library [1]. Repeated attempts to obtain the full-length clone by homology probing with the partial clone described above were unsuccessful. Therefore, a full-length clone encoding human Kv2.1 was assembled using portions of the rat Kv2.1 cDNA. Predicted rat and human Kv2.1 amino acid sequences differ in 51 residues, with two differences in the N-terminal regions, 49 differences in the C terminus, and complete identity in the putative transmembrane regions, S1–S6. Since we were only missing the N terminus and a portion of the transmembrane segments of hKv2.1, we mutated the N-terminal coding portion of rat Kv2.1 to the human Kv2.1 coding sequence and ligated it to the partial hKv2.1 clone. The conversion of rat to human Kv2.1 in the N-terminal coding region (Q71E and E79D) was performed by PCR mutagenesis by overlap extension [8]. Rat Kv2.1 plasmid served as the template in a PCR with single sense and antisense oligonucleotides (51 bases) encompassing both residue changes in combination with appropriate flanking oligonucleotides. The PCR product generated by the overlap method was cloned in pCR_{II} (Invitrogen) for sequencing, and the two changes from rat to human Kv2.1 coding sequence were verified. The complete hKv2.1 coding sequence was assembled from three partial fragments as follows. A portion of the rat to human Kv2.1 cDNA from the PCR above was cut from pCR_{II} with *NotI* (cutting in the pCR_{II} vector, 5' to the start codon) and *ClaI* (cutting at bp 359 in rat Kv2.1). The middle piece was a *ClaI/HpaI* fragment cut from rat Kv2.1 (the *HpaI* site is in the S6 region of rat Kv2.1). The amino acid sequence specified by this rat fragment is identical to the human Kv2.1 predicted sequence. The third piece consisted of a portion of the hKv2.1 fragment (*HpaI/EcoRI*). A *HpaI* site in S6 was introduced into hKv2.1 by PCR, and the *EcoRI* site was in the plasmid flanking the stop codon. The three fragments were ligated to a *NotI/EcoRI* cut derivative of pCR_{II}, A⁺-pCR_{II} [19] for synthesis of cRNA to test for functional expression in *Xenopus* oocytes. This full-length hKv2.1 construct generated large delayed-rectifier currents in *Xenopus* oocytes.

For heterologous expression in mammalian cells, the hKv2.1 construct was subcloned into the mammalian expression vector pcDNA3 (Invitrogen). The human glioblas-

toma cell line, U-373 MG, (obtained from ATCC) was transfected with the hKv2.1/pcDNA3 construct using previously described techniques [4]. This cell line was chosen for its superior ability to adhere to the glass coverslips upon which all electrophysiological recordings were carried out. Antibiotic resistant clones were screened electrophysiologically for hKv2.1 currents.

2.2. RNase protection

A fragment (360 bp) encoding the unique C-terminal 120 residues of hKv2.1 was prepared by PCR and cloned into pCR_{II} (Invitrogen) to be used as the template to prepare an hKv2.1-specific probe for RNase protection assays. The fragment was sequenced to confirm that no mutations were introduced by PCR, and to determine the orientation in the pCR_{II} vector. Plasmid DNA was purified on Qiagen Midi-Prep plasmid purification columns, and linearized with *HindIII*. 32 P-Labeled antisense transcripts were prepared from linearized template with T7 RNA polymerase using the MAXIscript Transcription kit (Ambion) according to the manufacturer's protocol. Full-length antisense transcripts (486 bases) were gel purified on a denaturing 5% polyacrylamide gel containing 8 M urea, and eluted from the gel slices by overnight incubation at 37°C in the following buffer: 0.5 mM ammonium acetate, 1 mM EDTA, 0.2% SDS. As a control, an antisense probe for human cyclophilin (139 bases) was prepared in similar fashion from a linearized template obtained from Ambion.

Total RNA from human atrial appendage, right ventricle, and left ventricle was isolated using RNA-STAT 60 (TEL-TEST). The ventricular tissue samples were obtained, in accordance with Tulane University School of Medicine Institutional guidelines, from the explanted heart of a 7-year-old female patient with dilated cardiomyopathy undergoing cardiac transplant. Human atrial appendage tissue was pooled from ten adult patients undergoing aorto-coronary bypass surgery. Total RNA from whole adult human brain was purchased from Clontech (No. 64020-1).

The RNase protection experiments were performed using the HybSpeed RPA kit (Ambion) following the manufacturer's protocol. Ten μ g of each total RNA sample was incubated with 20 000 cpm of hKv2.1 probe and 2000 cpm of human cyclophilin probe for 20 min at 68°C. As a control, the probes were also incubated with 10 μ g of yeast tRNA. The hybridization mixtures were then digested for 45 min with ribonuclease T1 at 37°C. Following RNase treatment, the protected fragments were precipitated, resuspended in gel loading buffer, and electrophoresed in a 5% polyacrylamide gel containing 8 M urea. The gel was dried and exposed to Kodak Biomax MS film for 8 h at –80°C.

2.3. RT-PCR

Human brain and heart poly(A)⁺RNA (Clontech) were used as templates in first strand cDNA synthesis reactions

using random hexamers and MuLV reverse transcriptase (Perkin-Elmer). Specifically, 100 ng of poly(A)⁺ RNA was incubated with random hexamers (250 nM) and cDNA synthesis (20 μ l reaction) was carried out using the manufacturer's protocol (GeneAmp RNA PCR kit, Perkin-Elmer) except that the reaction time at 42°C was increased to 1 h. As a control, reactions were performed in the absence of reverse transcriptase as well. Ten μ l of each cDNA synthesis reaction was used as template in the PCR reaction. The two oligos for the Kv2.1 PCR were: 5'-GAATGTCCGCCGCGTGGTCCAG-3' (sense) and 5'-CT-TGGCTCTCTCCAGAGCCTC-3' (antisense). These correspond to bp 927–948 and bp 1357–1377, respectively, in the human Kv2.1 clone (accession No. X68302). The oligos flank the S4–S6 region of the channel and generate a PCR product of 450 bp. For comparison to Kv2.1, we performed PCR on a portion of the Kv1 accessory subunit, hKv β 2, using the following oligos: 5'-ATCTACAG-TACTCGGTATGGGAGTC-3' (sense) and 5'-CCTC-CATGATCTCCATGGAGC-3' (antisense). These oligos correspond to bp 104–128 and bp 606–626, respectively, of the human Kv β 2 sequence (accession No. U33429) and generate a 522 bp PCR product. PCR (50 μ l final volume) was carried out with the GeneAmp PCR Kit (Perkin-Elmer) using 35 cycles of the following program: 94°C, 30 s; 55°C, 30 s; 72°C, 30 s. Ten μ l of each PCR was analyzed on an ethidium bromide stained agarose gel.

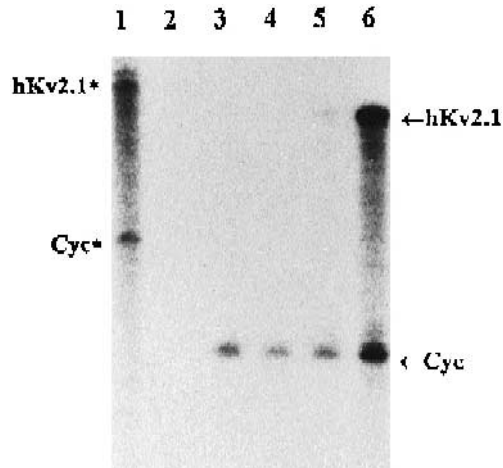


Fig. 1. RNase protection analysis of hKv2.1 expression in human atrium, ventricle, and brain. Control probe and protected fragments were electrophoresed on a 5% acrylamide/8 M urea denaturing gel, and autoradiographed. Lane 1 shows the full-length hKv2.1 (486 bases) and cyclophilin (cyc) (139 bases) probe fragments (unhybridized and undigested). Lane 2 corresponds to a control hybridization and RNase digestion carried out in the presence of probe and yeast tRNA only. Lanes 3, 4, 5, and 6 correspond to protected hKv2.1 (360 bases) and human cyclophilin (103 bases) fragments in total RNA from human atrial appendage tissue (lane 3), right ventricle (lane 4), left ventricle (lane 5), and whole brain (lane 6).

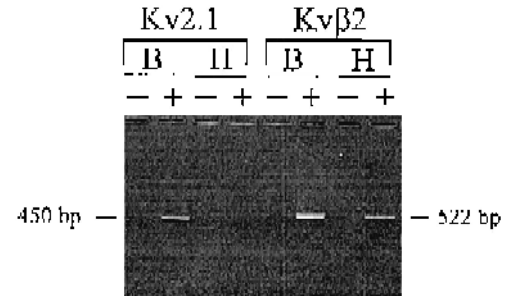


Fig. 2. RT-PCR analysis of hKv2.1 expression in human heart and brain. The left panel (labeled Kv2.1) shows the results from RT-PCR using oligos flanking a portion of human Kv2.1 sequence using human brain (B) or heart (H) poly(A)⁺ RNA as template. Reactions were done in the absence (-) or presence (+) of reverse transcriptase. Note the appearance of a 450 bp band only from brain. As a control, RT-PCR of a portion of hKv β 2 sequence from human brain (B) and heart (H) is shown in the right panel. A PCR band of the expected size (522 bp) is detected in both brain and heart.

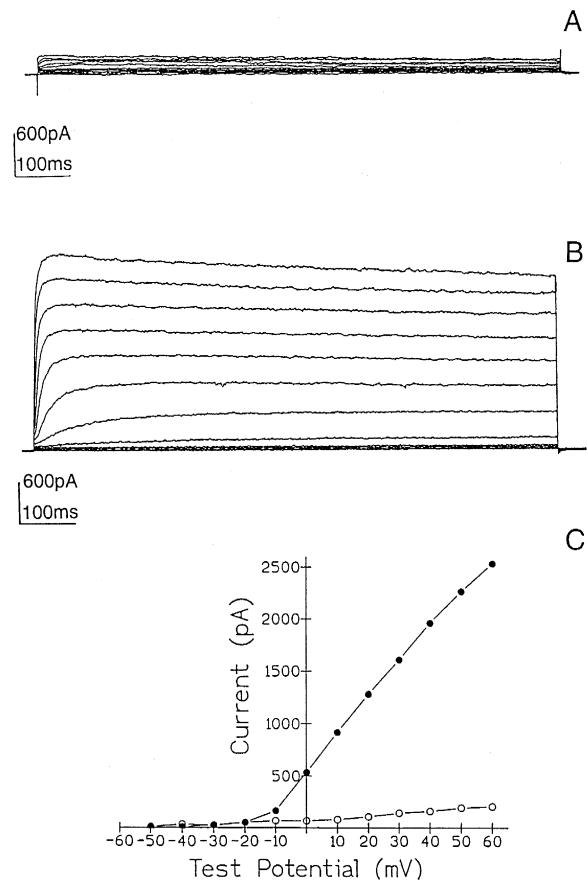


Fig. 3. Current-voltage relationship for Kv2.1. Current traces from a control (untransfected) glioblastoma cell (A) or one transfected with the cDNA encoding hKv2.1 (B) are shown. Currents were elicited by 1 s clamp pulses ranging from -50 mV to +60 mV in 10 mV increments from a holding potential of -80 mV. The resultant I-V relationships for the control cell (open circles) and the transfected cell (filled circles) are shown in C.

2.4. Electrophysiological experiments

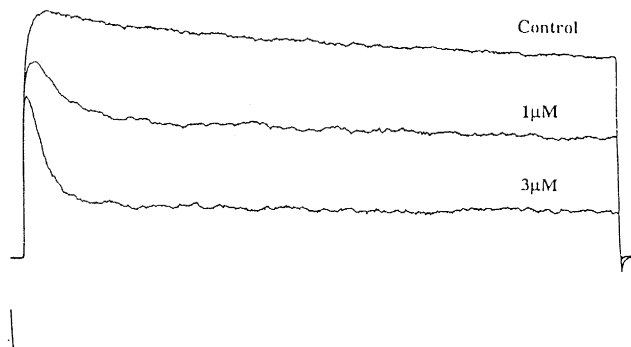
Cells used for electrophysiological recordings were seeded on glass coverslips 24–72 h prior to use. Small, spherical cells, approx. 10 μm in diameter, were used for all recordings. Whole-cell and inside-out membrane patch recordings were made at room temperature via the gigaseal patch-clamp technique as described by Hamill et al. [7] using an Axopatch-1D amplifier (Axon Instruments, Foster City, CA). Electrodes were fashioned from TW150F glass capillary tubes (World Precision Instruments, New Haven CT) and had resistances of 2–3 $\text{M}\Omega$ when filled with internal solution of the following composition (mM): potassium aspartate, 120; KCl, 20; Na_2ATP , 4.0; HEPES, 5.0; MgCl_2 , 1.0; pH 7.2 with KOH. This served as the external solution for inside-out membrane patch recordings. The external solution contained (in mM): NaCl, 130; KCl, 5.0; sodium acetate, 2.8; MgCl_2 , 1.0; HEPES, 10; glucose, 10; CaCl_2 , 1.0; pH 7.4 with 1 N NaOH. This served as the internal solution for inside-out membrane patch recordings. Series resistance was compensated following rupture of the seal, to provide the fastest possible capacity transient without ringing. Currents were sampled at 1 kHz and filtered at 500 Hz unless otherwise stated. All currents were corrected on-line using the P/4 subtraction method except where otherwise noted. Electrophysiologi-

cal data were analyzed using Clampfit in pCLAMP software (Axon Instruments). IC_{50} values for all compounds were determined by non-linear regression analyses using GraphPAD software (San Diego, CA). For steady-state activation and inactivation curves, data were normalized and fit to the Boltzman equation: $[1 + \exp((V_{0.5} - V)/k)]^{-1}$ where V is the membrane voltage, $V_{0.5}$ is the midpoint of the curve and k is the slope factor. All compounds were obtained from commercial sources.

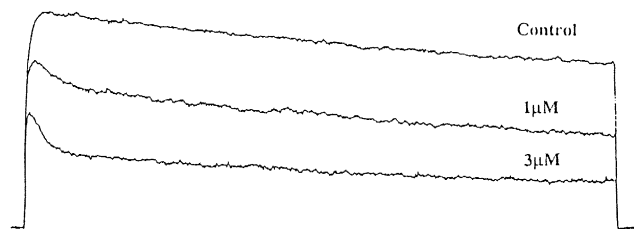
3. Results

In rat, Kv2.1 transcripts have been found in both rat brain [3] and rat heart tissue [2,3] suggesting that Kv2.1 channels may contribute to K^+ currents in these tissues. We examined the expression of hKv2.1 transcripts in human brain and heart by RNase protection analysis (Fig. 1), and found that while there were abundant transcripts in adult whole brain, there was virtually no Kv2.1 gene expression detected in either human atrium or ventricle. This is in marked contrast to the situation in rat heart in which Kv2.1, along with Kv1.2, Kv1.4, Kv1.5, and Kv4.2, constitute the most abundant voltage-gated K^+ channel transcripts [2]. The detection of human cyclophilin transcripts in human atrium and ventricular RNA, however,

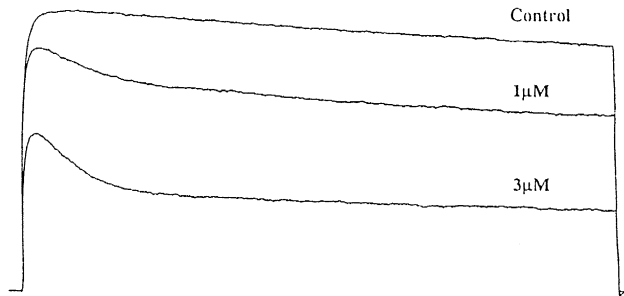
A Trifluoperazine



B Trifluoperidol



C Pimozide



D

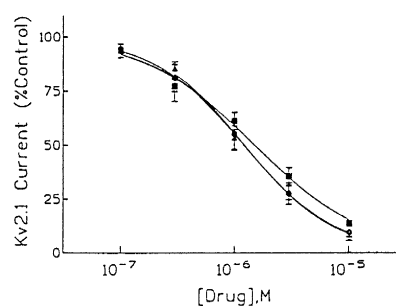


Fig. 4. Inhibition of hKv2.1 current by antipsychotic agents. Whole cell hKv2.1 currents were elicited by 1 s depolarizing pulses to +40 mV from a holding potential of -80 mV. The effects of trifluoperazine, trifluoperidol and pimozide are shown in A, B, and C, respectively. D: dose-response relationships for trifluoperazine ($\text{IC}_{50} = 1.21 \mu\text{M}$, circles) trifluoperidol ($\text{IC}_{50} = 1.51 \mu\text{M}$, squares) and pimozide ($\text{IC}_{50} = 1.23 \mu\text{M}$, triangles) are shown. Error bars indicate S.E.M. ($n = 3-5$). Calibration bars represent 400 pA and 100 ms.

indicates that the samples were not lost during the experiment. Consistent with data from rat heart, cyclophilin transcripts are more abundant in brain relative to atrium and ventricle [2].

To confirm the absence or low level of Kv2.1 expression in human heart, we performed RT-PCR reactions using human brain and heart poly(A)⁺ RNAs as template. For Kv2.1 PCR, we chose oligos that flank the S4 and S6 domains, a region different from that used in the RNase protection assay. As shown in Fig. 2, a PCR product of the expected size was visible only in the sample derived from

brain. To ensure that the quality of the human heart RNA equaled that of the brain, we performed control reactions using oligos flanking a region of an unrelated gene, hKv β 2, an accessory subunit for the Kv1 subfamily. Here we observed 522 bp PCR products from both brain and heart confirming that the lack of Kv2.1 in human heart was not due to poor quality of heart RNA. Thus, these results confirm the absence or, at least, the very low level of expression of Kv2.1 in human heart.

We next examined the functional properties of the hKv2.1 channel after stable transfection into the human

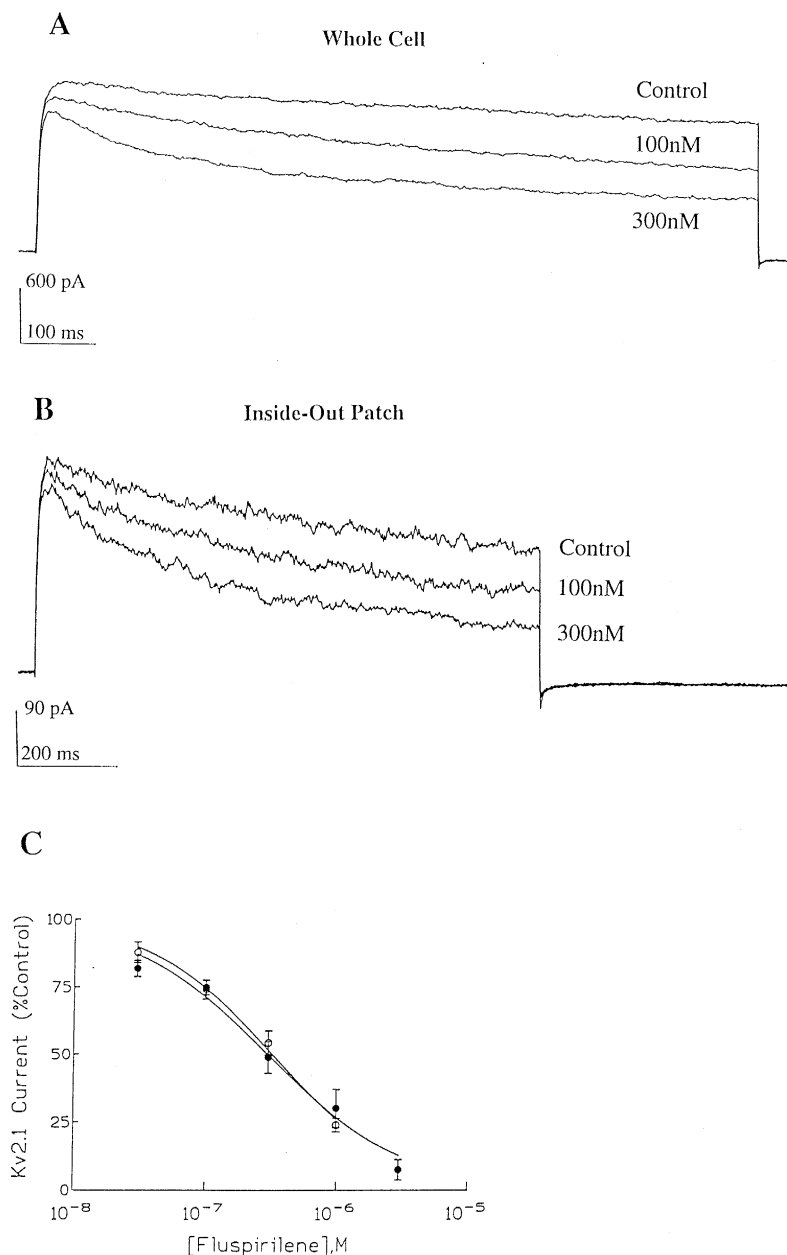


Fig. 5. Effects of fluspirilene on hKv2.1 current. Currents were elicited by 1 s test depolarizations to +40 mV from a holding potential of -80 mV in both the whole cell (A) and inside-out membrane patch (B) configuration. The effects of 100 and 300 nM fluspirilene are indicated. C: dose-response relationships for whole cell (filled circles) and inside-out patch data (open circles) yielded IC₅₀ values of 297 nM and 321 nM, respectively. Error bars indicate S.E.M. ($n = 3-9$).

glioblastoma cell line. Untransfected cells displayed small outward currents which averaged 106 ± 23 pA when measured at +40 mV ($n = 13$, Fig. 3A). In contrast, cells stably transformed with the cDNA encoding hKv2.1 displayed large sustained outward currents which activated at membrane potentials positive to -30 mV and ranged in amplitude from several hundred picoamperes to greater than 20 nA at +40 mV (Fig. 3B and C). Cells with current amplitudes ranging from 1.5 to 4.0 nA at +40 mV (average current density = 305 ± 26 pA/pF, $n = 19$) were used throughout this study. These currents exhibited slow activation kinetics with time constants ranging from 75.7 ± 8.1 ms at 0 mV to 6.9 ± 0.7 ms at +60 mV ($n = 6$). Steady-state activation parameters were determined from outward tail currents recorded at -45 mV following 100 ms depolarizing pulses to potentials ranging from -60 mV to +60 mV. Tail current amplitudes were extrapolated from a single exponential fit of the tail current decay. The resultant steady-state activation curve yielded a half-activation value ($V_{0.5}$) of 4.7 ± 3.9 mV and a slope value (k) of 8.4 ± 0.8 mV ($n = 5$). Finally, hKv2.1 current was inhibited by the classical K^+ channel blocker tetraethylammonium with an IC_{50} value of 3.63×10^{-3} M.

We examined the effects of several antipsychotic agents on hKv2.1 channel current. The structurally distinct dopamine receptor antagonists trifluoperazine, trifluoperidol and pimozide each inhibited hKv2.1 current. This inhibi-

tion was apparent at drug concentrations of 300 nM or higher. All three compounds suppressed peak hKv2.1 current measured at a test potential of +40 mV (Fig. 4A–C). In addition, each drug also enhanced the rate of hKv2.1 current decay during the depolarizing pulse. Finally, the IC_{50} values for these compounds were also similar measuring 1.20, 1.51 and 1.23 μ M for trifluoperazine, trifluoperidol and pimozide, respectively (Fig. 4D).

The effects of the diphenylbutylpiperidine fluspirilene on hKv2.1 current are illustrated in Fig. 5. We found that fluspirilene was severalfold more potent than the other antipsychotic agents tested at inhibiting hKv2.1 current. Potency was similar whether hKv2.1 current was recorded in the whole-cell mode ($IC_{50} = 297$ nM) or using cell-free inside-out membrane patches ($IC_{50} = 321$ nM). Application of fluspirilene resulted in a small reduction in peak current accompanied by an acceleration in the rate of current decay. In the absence of drug, hKv2.1 current showed little decay during the course of a 1 s step depolarization to +40 mV. In the presence of fluspirilene current decay was accelerated and its time course was well fitted to a single exponential function. These effects were concentration dependent with time constants ranging from 484 ± 37 ms ($n = 4$) at a concentration of 100 nM to 78 ± 16 ms ($n = 3$) in the presence of 3 μ M fluspirilene under whole-cell recording conditions. Furthermore, the effects of fluspirilene on hKv2.1 were largely reversible

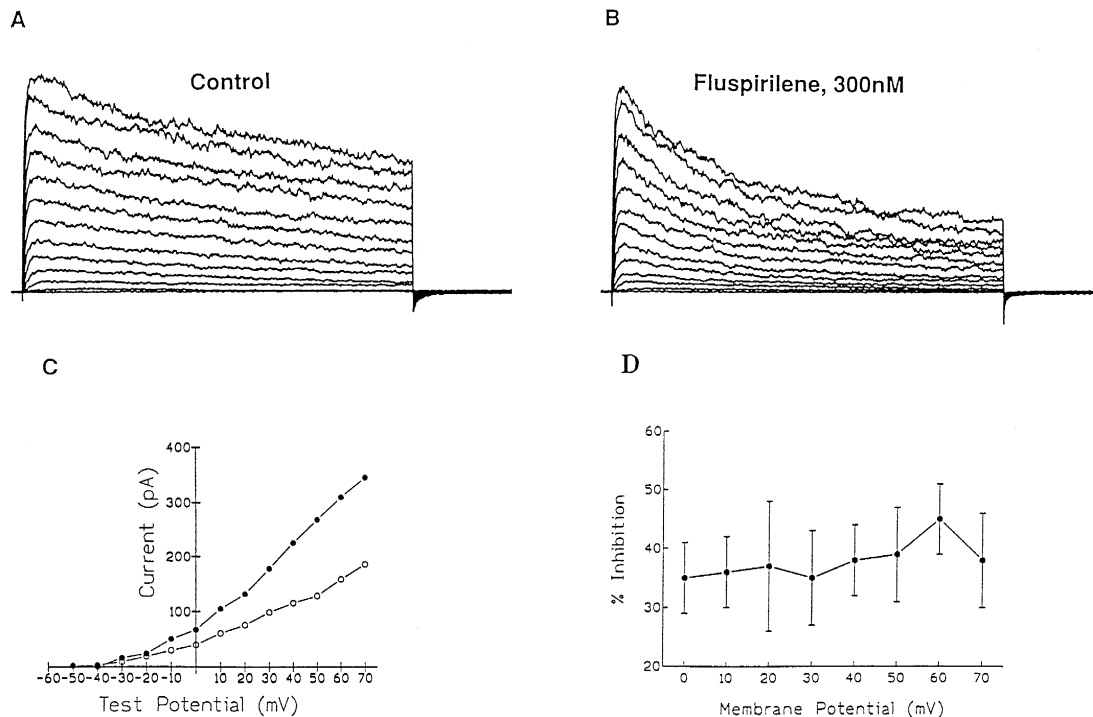


Fig. 6. Effects of fluspirilene on the hKv2.1 I-V relationship. Currents were elicited from an inside-out membrane patch by 1 s test depolarizations to various potentials from a holding potential of -80 mV. Traces in the absence and presence of 300 nM fluspirilene are shown in panels A and B, respectively. The resultant I-V relationships in the absence (filled circles) and presence (open circles) of 300 nM fluspirilene are shown in C. The last 100 ms of each trace were averaged to generate the I-V plots. D: the percent inhibition of hKv2.1 current by fluspirilene is plotted against test potential. Bars indicate S.E.M. ($n = 4$).

following prolonged (15–20 min) washout of the drug (data not shown). Although fluspirilene enhanced the rate of hKv2.1 current decay, it had no effect on either current activation or deactivation. In the absence of drug, hKv2.1 current activated with a time constant that averaged 9.56 ± 1.52 ms at +40 mV ($n = 5$). In the presence of $1 \mu\text{M}$ fluspirilene this value was not significantly changed and measured 7.98 ± 1.45 ms ($n = 5$). Likewise, fluspirilene had no significant effect on hKv2.1 current deactivation. When fitted to a single exponential function, the time constant of outward tail currents measured at -45 mV averaged 14.61 ± 1.66 ms ($n = 5$) under control condi-

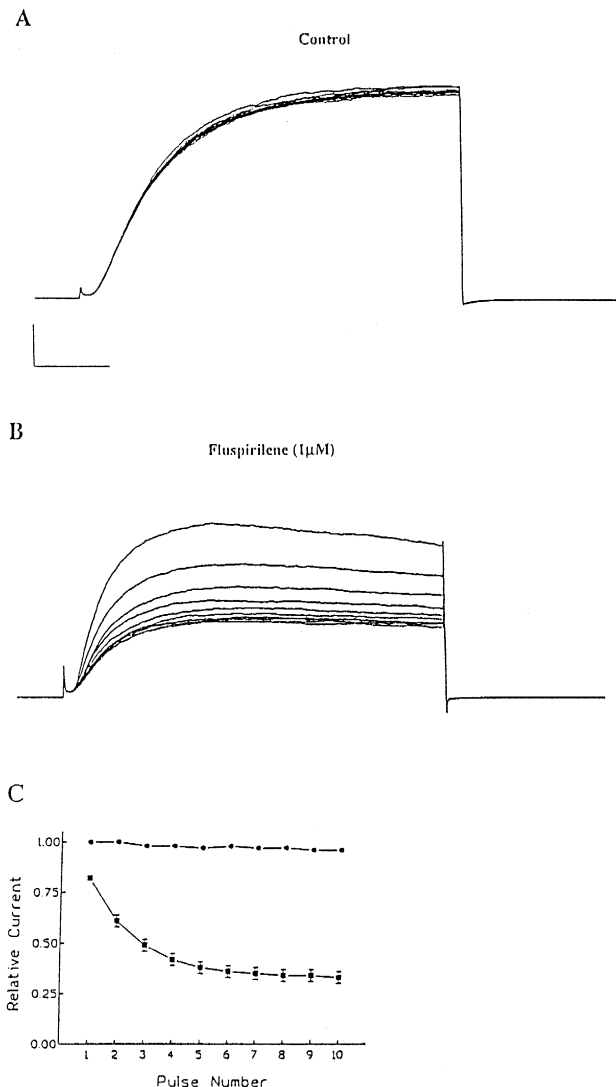


Fig. 7. Frequency-dependent effects of fluspirilene on hKv2.1. Cells were held at -80 mV and a train of ten depolarizing pulses to $+40$ mV (100 ms duration) was delivered at a rate of 2 Hz. Traces in the absence and presence of $1 \mu\text{M}$ fluspirilene are shown in panels A and B, respectively. Peak hKv2.1 current in the absence (circles) and presence (squares) of $1 \mu\text{M}$ fluspirilene is plotted against pulse number in panel C. C: currents are expressed relative to the peak current during pulse No. 1. Current traces were not leak corrected. Error bars indicate S.E.M. ($n = 4$). Calibration bars represent 900 pA and 20 ms.

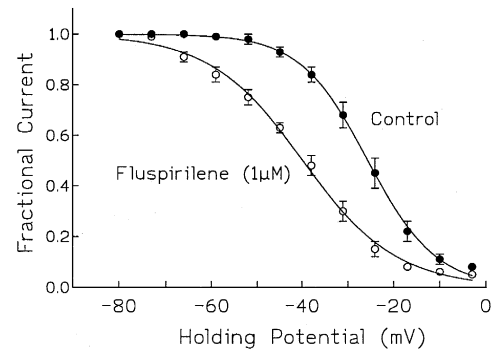


Fig. 8. Effects of fluspirilene on the steady-state inactivation properties of hKv2.1. Steady-state inactivation curves were constructed as described in the text. Data were normalized to the current amplitude evoked from a holding potential of -80 mV. The midpotential ($V_{0.5}$) and slope (k) values in the absence of fluspirilene (filled circles) measured -25.6 ± 1.4 mV and -7.3 ± 0.9 mV, respectively. In the presence of $1 \mu\text{M}$ fluspirilene these values measured -40.0 ± 1.5 mV and -10.2 ± 0.3 mV, respectively. Error bars indicate S.E.M. ($n = 4$).

tions. In the presence of $1 \mu\text{M}$ fluspirilene this value averaged 16.11 ± 1.42 ms ($n = 5$).

Fig. 6 shows the effects of fluspirilene on hKv2.1 current from an inside-out membrane patch recorded over a wide range of test potentials. Current traces in the absence and presence of 300 nM fluspirilene are illustrated in Fig. 6A and B, respectively. The resultant current-voltage (I-V) relationships for this data are presented in Fig. 6C. As can be seen, fluspirilene produces time-dependent inhibition of hKv2.1 current over a wide range of membrane potentials. However, no significant voltage dependence of channel block was observed (Fig. 6D).

We next examined whether fluspirilene displayed any frequency-dependent effects on hKv2.1 current. Frequency dependence was assessed by applying a train of 100 ms depolarizing pulses to $+40$ mV from a holding potential of -80 mV at a rate of 2 Hz. Under these conditions peak current in the absence of drug was not significantly altered over the course of ten repetitive depolarizing pulses (Fig. 7A and C). Under the same conditions peak hKv2.1 current was decreased by $67 \pm 3\%$ in the presence of $1 \mu\text{M}$ fluspirilene (Fig. 7B and C). This decrease was significantly different from control values ($P < 0.05$ analysis of variance with least significant difference test).

The effects of fluspirilene on the steady-state inactivation properties of hKv2.1 are illustrated in Fig. 8. Inactivation curves were constructed by measuring current evoked by depolarizing pulses to $+40$ mV while the holding potential (20 s duration) was increased in 7 mV increments from -80 mV to -3 mV. Fig. 8 shows the steady-state inactivation curves in the absence and presence of $1 \mu\text{M}$ fluspirilene. In the absence of drug the midpotential ($V_{0.5}$) and slope value (k) of the steady-state inactivation curve measured -25.6 ± 1.4 mV and -7.3 ± 0.9 mV, respectively. In the presence of $1 \mu\text{M}$ fluspirilene these values were significantly ($P < 0.05$) changed with $V_{0.5}$ and k

values measuring -40.0 ± 1.5 mV and -10.2 ± 0.3 mV, respectively.

4. Discussion

We report here the stable heterologous expression of the human voltage-gated K^+ channel, hKv2.1, in the human cell line, glioblastoma U-373 MG. A partial cDNA encoding hKv2.1 from the middle of the S4 transmembrane segment through the terminal stop codon was obtained from a human brain cDNA library, and was identical in sequence to the corresponding clone isolated from a human genomic DNA library [1]. We constructed a full-length hKv2.1 coding sequence by ligating the missing fragment, derived from rat Kv2.1 cDNA which was mutated to encode the two amino acid residues that differ in the human sequence, to the human partial clone. Cells transformed with hKv2.1 express large outward currents with relatively little contamination by endogenous currents. The time constant for channel activation at 0 mV, TEA sensitivity and steady-state activation characteristics recorded here are similar to those described for the transient expression of hKv2.1 in oocytes [1], while the midpotentials of both the steady-state activation and inactivation curves are, by comparison, approx. 5–10 mV more depolarized than those recorded following the direct microinjection of hKv2.1 cRNA into mouse fibroblasts or rat leukemia cells [9].

Through RNase protection analysis, hKv2.1 transcripts were easily detected in whole adult brain RNA but virtually undetectable in total RNA from human heart, both atrium and ventricle. The absence of hKv2.1 expression in human heart was further confirmed using RT-PCR. This is in marked contrast to the pattern of Kv2.1 expression in other species. In the rat, for example, Kv2.1 was cloned from heart [17], and Northern blotting has shown that Kv2.1 transcripts are far more abundant in mRNA from heart compared to whole brain in both neonatal and adult tissue [3]. In addition, RNase protection experiments have identified Kv2.1 as one of the predominant voltage-gated K^+ channel transcripts in rat heart with a slightly greater expression in ventricle relative to atrium [2]. The data presented here provide a molecular correlate to other electrophysiological studies which have also failed to demonstrate Kv2.1-like currents in human ventricular cells [13]. This species-dependent expression of Kv2.1 (as well as other K^+ channels) has important implications for drug development, especially in predicting the tissue selective nature and toxicological profiles of compounds prior to their clinical evaluation. For example, drugs that specifically interact with hKv2.1 may not be expected to have cardiac effects due to the very low expression of this channel in various human cardiac tissues. Further investigation of the distribution and relative abundance of ion channel subtypes in human tissues should prove valuable.

We tested a number of antipsychotic drugs for their ability to interact with hKv2.1. The structurally diverse dopamine antagonists trifluoperazine, trifluoperidol and pimozide inhibited Kv2.1 current with IC_{50} values of approx. 1 μ M, while fluspirilene, a diphenylbutylpiperidine similar to pimozide, was 4–5-fold more potent than these agents at blocking hKv2.1 channel currents. Indeed, small but consistent blockade of hKv2.1 was observed with fluspirilene concentrations as low as 30 nM. These and other antipsychotic agents are known to interact with several distinct classes of voltage-dependent Ca^{2+} channels resulting in functional block of these channels over a concentration range of approx. 100 nM–10 μ M [6,12,18]. In fact, diphenylbutylpiperidines such as pimozide and fluspirilene are thought to represent a distinct class of L-type Ca^{2+} channel antagonist [11,20]. The present data support a role for these antipsychotic agents as effective blockers of hKv2.1. Interactions with hKv2.1 and possibly other voltage-dependent K^+ channels should be considered when these drugs are employed in this concentration range. It is possible that these compounds may recognize homologous binding domains in both the Ca^{2+} channels and hKv2.1 in a manner similar to that previously described for the interaction of the Ca^{2+} antagonist verapamil with the human cardiac K^+ channel Kv1.5 [16].

Although their interaction with Ca^{2+} channels has been well described, comparatively little is known about the mechanisms by which antipsychotic agents act to block voltage-dependent K^+ channels. A recent report has demonstrated that the diphenylbutylpiperidines haloperidol and fluspirilene can produce tonic block of K^+ currents in rat pheochromocytoma with IC_{50} values of approx. 10 μ M [14]. By comparison we find that fluspirilene is a far more potent antagonist of the human brain K^+ channel Kv2.1. The blocking effects of fluspirilene were both time- and frequency-dependent but independent of membrane voltage. Furthermore, the drug had no effect on the kinetics of Kv2.1 current activation or deactivation. However, fluspirilene produced a hyperpolarizing shift in the hKv2.1 inactivation curve. This finding suggests that at least some of the blocking effects of fluspirilene may be due to an interaction with the inactivated state of the hKv2.1 channel. Further studies utilizing single channel recordings will be necessary to determine the exact mechanism of action of fluspirilene on hKv2.1.

In summary, we have described some of the functional and pharmacological properties of the human Kv2.1 K^+ channel stably expressed in a glioblastoma cell line. mRNA levels of hKv2.1 were abundant in human brain but virtually absent in various human cardiac tissues. Cells transformed with hKv2.1 display currents with biophysical properties that are generally similar to those previously described for the transient expression of hKv2.1. A variety of antipsychotic agents were shown to block hKv2.1 with fluspirilene being the most potent in this regard. The effects of fluspirilene were both time- and frequency-de-

pendent and resulted in a hyperpolarizing shift in the hKv2.1 steady-state inactivation relationship. Further pharmacological studies utilizing stable expression systems like the one described here should facilitate the development of new agents which modulate hKv2.1 activity. Such compounds could find use in the treatment of neurological disorders.

Acknowledgements

The authors would like to thank Drs. Theresa Roca and John Pigott, Tulane University School of Medicine, for their help in obtaining human cardiac tissue.

References

- [1] B. Albrecht, C. Lorra, M. Stocker, O. Pongs, Cloning and characterization of a human delayed rectifier potassium channel gene, *Recept. Channels* 1 (1993) 99–110.
- [2] J.E. Dixon, D. MacKinnon, Quantitative analysis of potassium channel mRNA expression in atrial and ventricular muscle of rats, *Circ. Res.* 75 (1994) 252–260.
- [3] J.A. Drewe, S. Verma, G. Frech, R.H. Joho, Distinct spatial and temporal expression patterns of K⁺ channel mRNAs from different subfamilies, *J. Neurosci.* 12 (1992) 538–548.
- [4] D. Fedida, B. Wible, Z. Wang, B. Fermi, F. Faust, S. Nattel, A.M. Brown, Identity of novel delayed rectifier current from human heart with a cloned K⁺ channel current, *Circ. Res.* 73 (1993) 210–216.
- [5] G.C. Frech, A.M.J. VanDongen, G. Schuster, A.M. Brown, R.J. Joho, A novel potassium channel with delayed rectifier properties isolated from rat brain by expression cloning, *Nature* 340 (1989) 642–645.
- [6] R.J. Gould, K.M.M. Murphy, I.J. Reynolds, S.H. Snyder, Antischizophrenic drugs of the diphenylbutylpiperidine type act as calcium channel antagonists, *Proc. Natl. Acad. Sci. USA* 80 (1983) 5122–5125.
- [7] O.P. Hamill, A. Marty, E. Neher, B. Sakmann, F.J. Sigworth, Improved patch clamp techniques for high resolution current recording from cells and cell-free membrane patches, *Pflügers Arch.* 391 (1981) 85–100.
- [8] S.N. Ho, H.D. Hunt, R.M. Horton, J.K. Pullen, L.R. Pease, Site-directed mutagenesis by overlap extension using the polymerase chain reaction, *Gene* 77 (1989) 51–59.
- [9] S.R. Ikeda, F. Soler, R.D. Zühlke, R.H. Joho, D.L. Lewis, Heterologous expression of the human potassium channel Kv2.1 in clonal mammalian cells by direct cytoplasmic microinjection of cRNA, *Pflügers Arch.* 422 (1992) 201–203.
- [10] L.Y. Jan, Y.N. Jan, Structural elements involved in specific K⁺ channel functions, *Annu. Rev. Physiol.* 54 (1992) 537–555.
- [11] V.F. King, M.L. Garcia, J.L. Shevell, R.S. Slaughter, G.J. Kaczorowski, Substituted diphenylbutylpiperidines bind to a unique high affinity site on the L-type-calcium channel, *J. Biol. Chem.* 264 (1989) 5633–5641.
- [12] V. Klöckner, G. Isenberg, Calmodulin antagonists depress calcium and potassium currents in ventricular and vascular myocytes, *Am. J. Physiol.* 253 (1987) H1601–H1611.
- [13] G.-R. Li, J. Feng, L. Yue, M. Carrier, S. Nattel, Evidence for two components of delayed rectifier K⁺ current in human ventricular myocytes, *Circ. Res.* 78 (1996) 689–696.
- [14] K. Nakazawa, K. Ito, S. Koizumi, Y. Ohno, K. Inoue, Characterization of inhibition by haloperidol and chlorpromazine of a voltage-activated K⁺ current in rat pheochromocytoma cells, *Br. J. Pharmacol.* 116 (1995) 2603–2610.
- [15] O. Pongs, Molecular biology of voltage-dependent potassium channels, *Physiol. Rev.* 72 (Suppl. 4) (1992) 69–88.
- [16] D. Rampe, B. Wible, D. Fedida, R.C. Dage, A.M. Brown, Verapamil blocks a rapidly activating delayed rectifier K⁺ channel cloned from human heart, *Mol. Pharmacol.* 44 (1993) 642–648.
- [17] S.L. Roberds, M.M. Tamkun, Cloning and tissue-specific expression of five voltage-gated potassium channel cDNAs expressed in rat heart, *Proc. Natl. Acad. Sci. USA* 88 (1991) 1798–1802.
- [18] D.W.Y. Sah, B.P. Bean, Inhibition of P-type and N-type calcium channels by dopamine receptor antagonists, *Mol. Pharmacol.* 45 (1994) 84–92.
- [19] M. Tagliatela, B.A. Wible, R. Caporaso, A.M. Brown, Specification of pore properties by the carboxyl terminus of inwardly rectifying K⁺ channels, *Science* 264 (1994) 844–847.
- [20] D.J. Triggle, D.A. Lang, R.A. Janis, Ca²⁺ channel ligands: structure-function relationships of the 1,4-dihydropyridines, *Med. Res. Rev.* 9 (1989) 123–180.